Adaptive Multilevel Methods in Three Space Dimensions

Folkmar Bornemann
Freie Universität Berlin, Fachbereich Mathematik, Arnimallee 2–6, D–1000 Berlin 33

Bodo Erdmann Ralf Kornhuber
Konrad–Zuse–Zentrum Berlin, Heilbronner Straße 10, D–1000 Berlin 31

Summary. We consider the approximate solution of selfadjoint elliptic problems in three space dimensions by piecewise linear finite elements with respect to a highly non–uniform tetrahedral mesh which is generated adaptively. The arising linear systems are solved iteratively by the conjugate gradient method provided with a multilevel preconditioner. Here, the accuracy of the iterative solution is coupled with the discretization error. As the performance of hierarchical bases preconditioners deteriorate in three space dimensions, the BPX preconditioner is used, taking special care of an efficient implementation. Reliable a–posteriori estimates for the discretization error are derived from a local comparison with the approximation resulting from piecewise quadratic elements. To illustrate the theoretical results, we consider a familiar model problem involving reentrant corners and a real–life problem arising from hyperthermia, a recent clinical method for cancer therapy.

1 Introduction

Let $\Omega \subset \mathbb{R}^3$ be a polyhedral domain. We consider elliptic boundary value problems in the variational form

$$\text{Find } u \in H_0^1(\Omega) \text{ such that } a(u,v) = \ell(v)\ ,\ v \in H_0^1(\Omega) \tag{1}$$

with a symmetric, $H_0^1(\Omega)$–elliptic bilinear form $a(\cdot,\cdot)$ defined by

$$a(v,w) = \int_\Omega \sum_{i,j=1}^{3} a_{i,j}\partial_i v \partial_j w \; dx \tag{2}$$

and some functional $\ell \in H^{-1}(\Omega)$. Of course, more general boundary conditions may be incorporated in the usual way.

In the presence of complicated space geometries, discontinuous coefficients etc., the numerical solution of this problem in *three* space dimensions requires a *sophisticated* reduction of the computational amount of work. Only then we can hope to break through the complexity barrier of many important problems of the natural sciences and technology. Here the concept of *adaptivity*, i.e., the automatic distribution of the nodes used in the discretization, becomes more and more important. Additionally, *multigrid* or *multilevel* methods should be used to provide an efficient solution of the arising linear system. In two space dimensions adaptivity has already quite a history, whereas the appearance of multilevel methods is still more recent. Among the most popular codes in this field there is NFEARS due to Mesztenyi and Rheinboldt [24], PLTMG due to Bank [3] which is based on the hierarchical basis multigrid method and KASKADE due to Deuflhard,Leinen and Yserentant [14], where the conjugate gradient method preconditioned by the hierarchical basis is utilized. It is well–known that the good properties of the hierarchical basis are restricted to the 2–D case so that for three space dimensions the BPX preconditioner proposed by Bramble, Pasciak and Xu [10] should be used.

It is the purpose of this paper to collect well–known results on 3–D mesh refinement [6, 18, 34] and the BPX preconditioner [7, 9, 10, 13, 25] and on the other hand to extend related results on 2D–a–posteriori error estimates [14] and the data structures of the adaptive finite element code KASKADE [23, 27, 28] to obtain an adaptive multilevel finite element code for the adaptive multilevel treatment of (1) in *three* space dimensions.

The following three sections are devoted to the description of mesh refinement, preconditioning and a–posteriori error estimation which are the basic modules of any adaptive multilevel method. Special care is paid to an efficient implementation of the BPX preconditioner. For a detailed description of the underlying data structures we refer to Erdmann and Roitzsch [15]. The performance of the code is illustrated by two numerical examples reported in the final section.

2 Local Refinement

A partition $\mathcal{T}$ of the computational domain $\Omega \in \mathbb{R}^3$ into tetrahedra is called triangulation. Throughout this paper we consider triangulations which are conforming in the sense that the intersection of two different tetrahedra $t, \bar{t} \in \mathcal{T}$ either consists of a common triangular face, a common edge, a common vertex or is empty.

Starting with an intentionally coarse triangulation $\mathcal{T}_0$ of Ω we want to produce a sequence $\mathcal{T}_0, \ldots, \mathcal{T}_j$ of increasingly fine triangulations by the successive refinement of certain tetrahedra on which the solution is deemed too inac-

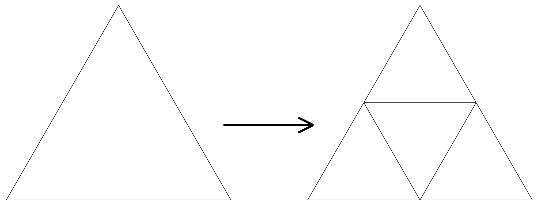

Figure 1. Regular Refinement of a Triangle

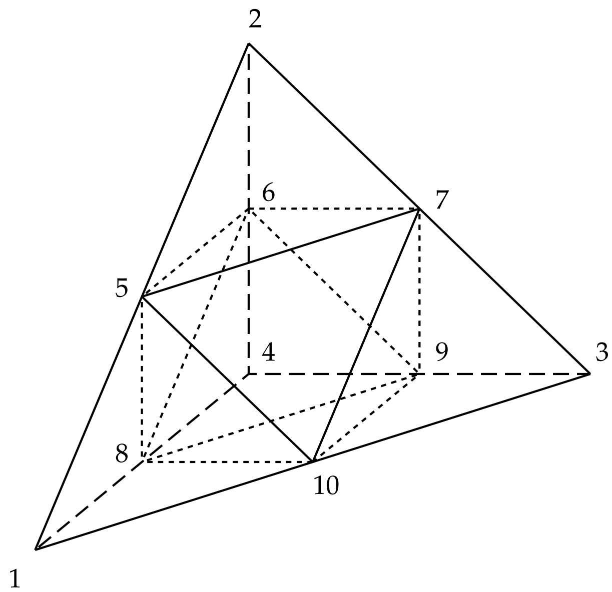

Figure 2. Regular Refinement of the Triangular Faces

curate. In this section we will consider the geometrical aspects of the local refinement referring to Section 3 for the a–posteriori estimates which govern the underlying selection process. In particular, we are interested in a refinement process which is stable in the following sense: For each $t \in \mathcal{T}_j$ the ratio of the diameter $\mathrm{diam}(t)$ and the radius of the largest interior ball $\rho(t)$ remains uniformly bounded, i.e.,

$$\sigma(t) = \mathrm{diam}(t)/\rho(t) \leq c\ , \quad t \in \mathcal{T}_j\ , \tag{3}$$

holds with a constant c independent of the refinement level j.

Extensions of the well-known regular (red) refinement of Bank and al. [4],

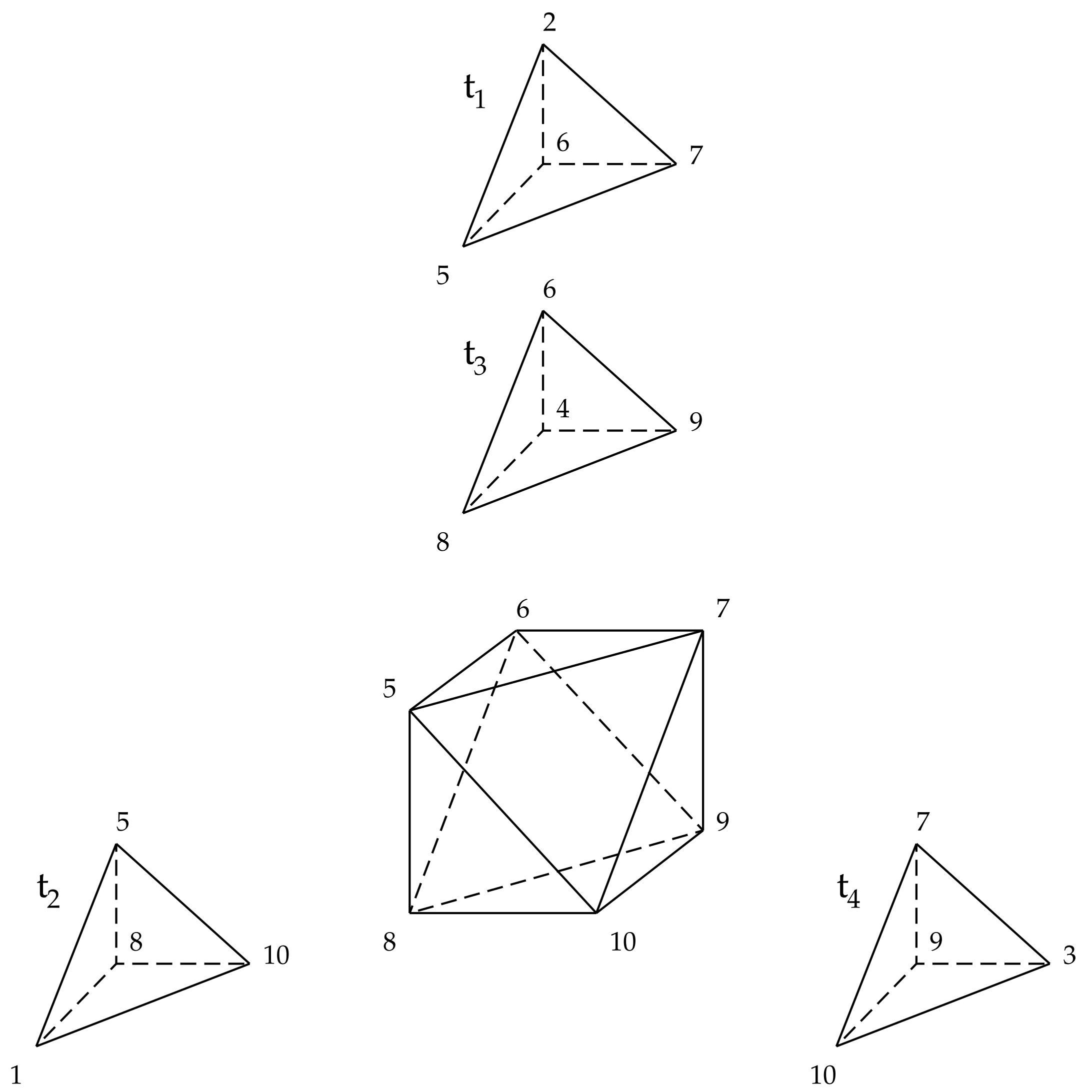

Figure 3. Four Tetrahedra and an Octahedron

depicted in Figure 1, to three space dimensions have been considered by various authors. We will briefly summarize the results of Zhang [34], Go Ong [18] and Bey [6]. Note that a related refinement was proposed by Bänsch [5]. By connecting the midpoints of the edges of a given tetrahedron t as shown in the Figure 2, we obtain four new tetrahedra $t_1, \ldots, t_4$ each of which corresponds to a vertex of t. Apart from these four tetrahedra there still remains an octahedron as illustrated in Figure 3. Note that this procedure provides a 2–D regular refinement of the triangular faces of t. We split the remaining octahedron in two pyramids each of which is separated in two tetrahedra. It is obvious from Figure 4 that the resulting splitting of the octahedron in four tetrahedra $t_5, \ldots, t_8$ is not unique, but depends on the selection of the interior diagonal of the octahedron which can be chosen in exactly three different ways. Each choice of this diagonal provides a regular refinement of the given tetrahedron t. One possibility is illustrated in Figure 5. There

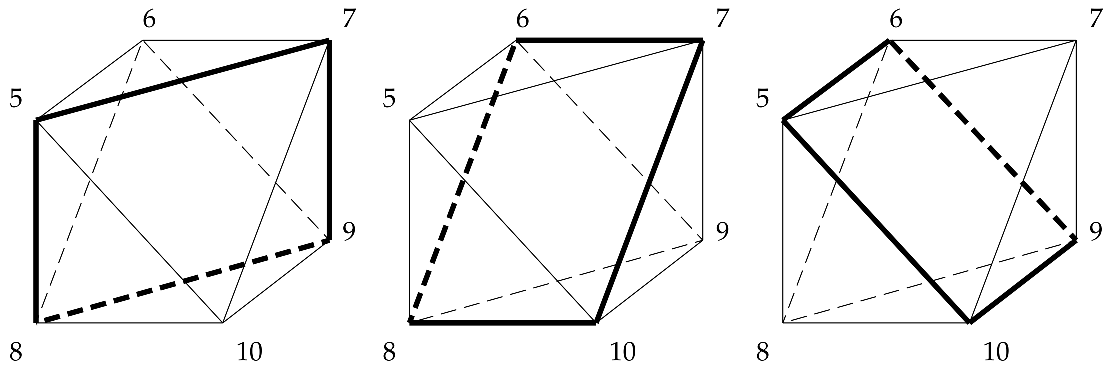

Figure 4. Splitting of the Remaining Octahedron in Two Pyramids

are well–known examples showing that successive regular refinement may be unstable in the sense of (3), if the diagonal interior edge is not selected properly [34].

However, it has been shown by Zhang [34] that the choice of the shortest diagonal leads to stable refinements if the triangular faces of the initial triangulation $\mathcal{T}_0$ have no obtuse angles. A strategy proposed by Go Ong [18] and Bey [6] relies on affine transformations to a reference tetrahedron and provides a stable regular refinement without any restrictions on $\mathcal{T}_0$. Note that in our numerical experiments both strategies lead to comparable results.

As in the 2–D case we use irregular (green) closures to obtain a conforming triangulation after the regular refinement of a proper subset of $\mathcal{T}_j$. In particular, we consider three different cases:

- Green-I: A tetrahedron with only one refined edge is bisected as shown in Figure 6.
- Green-II: A tetrahedron with two refined edges is divided into three or four tetrahedra as shown in Figure 7.
- Green-III: A tetrahedron with three refined edges of the same triangular face is divided into four tetrahedra as shown in Figure 8.

Note that irregular refinement does not introduce new nodal points.

In order to describe a complete refinement step we use the following denotations. As usual, a refined tetrahedron is said to be the father of its sub–tetrahedra, which in turn are called sons. We define the depth of a tetrahedron as the number of its ancestors. Finally, a tetrahedron is called regular if it is either contained in $\mathcal{T}_0$ or is resulting from regular refinement. Otherwise it is called irregular.

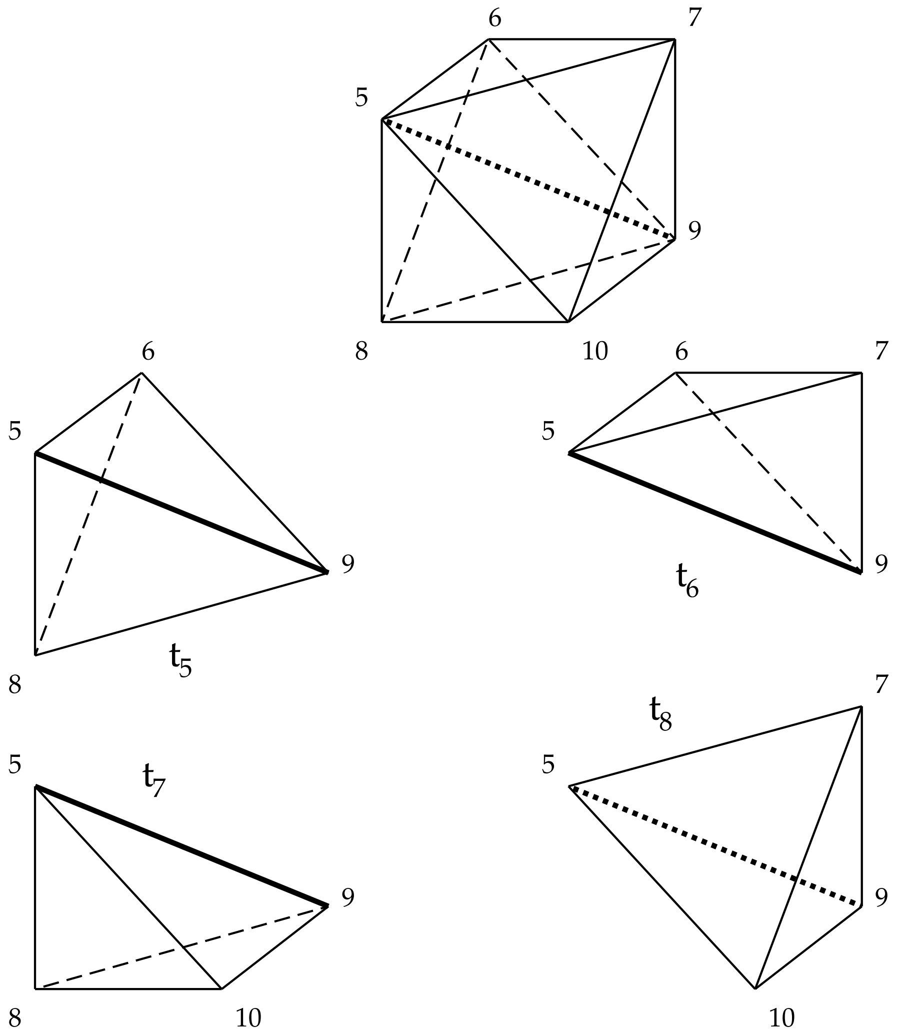

Figure 5. Splitting of the Remaining Octahedron in Four Tetrahedra Based on the Diagonal (5,9)

Now assume that a subset $\bar{\mathcal{T}}_j \subset \mathcal{T}_j$ has been marked for refinement based on some selection process. To preserve the stability (3) of the refinement process irregular tetrahedra must not be further refined. Hence, all green refinements are skipped replacing irregular tetrahedra contained in $\bar{\mathcal{T}}_j$ by their fathers. After the regular refinement of all $t \in \bar{\mathcal{T}}_j$, there may exist tetrahedra

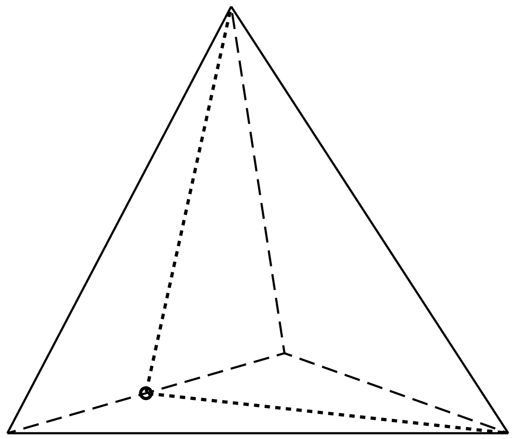

Figure 6. Green-I Closure

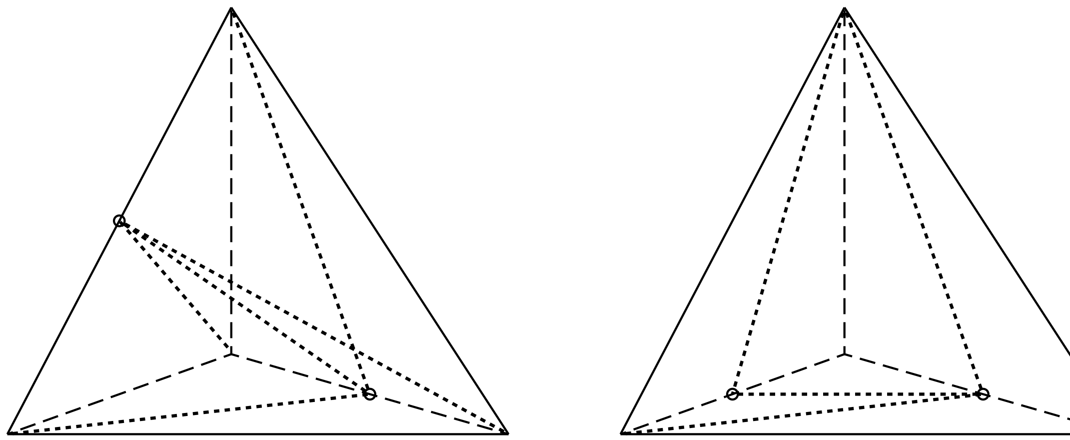

Figure 7. Green-II Closure

with edges which are refined twice or with three or more bisected edges corresponding to different triangular faces. Regular refinement is continued until no such tetrahedra are left. Now the remaining nonconforming vertices are remedied by green closure.

Extending the well–known data structures from the 2–D case [15], the triangu-

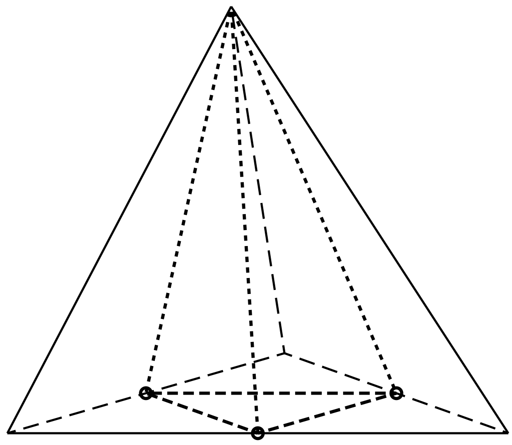

Figure 8. Green-III Closure

lations produced by this dynamic refinement process are stored as a sequence $\mathcal{T}_0, \ldots, \mathcal{T}_j$ with the properties:

(T1) Each vertex of $\mathcal{T}_{k+1}$ which does not belong to $\mathcal{T}_k$, is vertex of a regular tetrahedron, $0 \leq k < j$.

(T2) Irregular tetrahedra have no sons.

(T3) The father of each tetrahedron $t \in \mathcal{T}_{k+1} \setminus \mathcal{T}_k$ has depth k, $0 \leq k < j$.

The rule (T3) allows for the reconstruction of the whole sequence $\mathcal{T}_0, \ldots, \mathcal{T}_j$ of triangulations from $\mathcal{T}_0$ and $\mathcal{T}_j$ alone and the first two rules have been already mentioned above. Note that j indicates the maximal depth and not the number of dynamic refinement steps. The properties (T1 - T3) are meanwhile standard in the framework of multilevel methods [8, 14, 21, 33].

3 Preconditioning

Assume that a nested sequence $\mathcal{T}_0, \ldots, \mathcal{T}_j$ of triangulations satisfying (T1 – T3) has been constructed. In this section we focus on the efficient iterative solution of the linear system resulting from the finite element discretization

$$\text{Find } u_j \in \mathcal{S}_j \text{ such that } a(u_j, v) = \ell(v) \ , \ v \in \mathcal{S}_j \qquad (4)$$

of the variational problem (1). Here we make use of the finite element spaces $\mathcal{S}_k \subset H_0^1(\Omega)$, $k = 0, \ldots j$, denoting the subspace of all functions which are linear on each tetrahedron $t \in \mathcal{T}_k$ and continuous on Ω.

In particular, we describe an efficient implementation due to Bornemann [7] of the well–known BPX preconditioner [10, 33, 9] in the case of highly nonuniform grids.
As a consequence of (T1 –T3) we have

$$\mathcal{S}_0 \subset \mathcal{S}_1 \subset \ldots \subset \mathcal{S}_j.$$

By $\mathcal{N}_k$ we denote the nodal points of $\mathcal{T}_k$ which do not belong to the boundary $\partial\Omega$. Let $\{\psi_1^k, \ldots, \psi_{n_k}^k\}$ be the *nodal basis* of the space $\mathcal{S}_k$. We arrange the nodal basis in such a way that for some $m_k \leq n_k$, $k > 0$,

$$\psi_1^k, \ldots, \psi_{m_k}^k \notin \mathcal{S}_{k-1}$$

and

$$\psi_{m_k+1}^k, \ldots, \psi_{n_k}^k \in \mathcal{S}_{k-1}.$$

This extends formally to $m_0 = n_0$. Note that the case $m_k = n_k$ corresponds to uniform refinement of $\mathcal{T}_{k-1}$ to $\mathcal{T}_k$ and the case $m_k < n_k$ to nonuniform refinement which will be usually the case. The members of the set

$$\Psi_k = \{\psi_1^k, \ldots, \psi_{m_k}^k\}$$

are just those nodal basis functions of depth k which are *new*, i.e., are generated by the refinement process. We call the unique nodal point x for which $\psi(x) = 1$ the *supporting point* of the nodal basis function ψ. Denoting the set of edges of $\mathcal{T}_k$ which are not part of the boundary $\partial\Omega$ by $\mathcal{E}_k$, we will use the subset $\bar{\mathcal{E}}_{k-1} = \mathcal{E}_{k-1} \backslash \mathcal{E}_k$ of those edges which have been bisected for $\mathcal{T}_k$. The following result is crucial for our implementation.

Lemma 1 *The nodal basis functions of* Ψ_k*,* $k \geq 1$*, are supported exactly by those nodal points of* $\mathcal{N}_k$ *which are vertices and midpoints of edges* $e \in \bar{\mathcal{E}}_{k-1}$*. The total number* $\sum_{k=0}^{j} m_k$ *of mutually different basis functions is bounded according to*

$$\sum_{k=0}^{j} m_k \leq (5n_j - 2n_0)/3.$$

Proof. The first part is an immediate consequence of the refinement rule (T1). For the second part denote the set of vertices and of midpoints of $\bar{\mathcal{E}}_{k-1}$ by $\mathrm{ver}(\bar{\mathcal{E}}_{k-1})$ and $\mathrm{mid}(\bar{\mathcal{E}}_{k-1})$, respectively. Hence we have

$$m_k = \#\mathrm{ver}(\bar{\mathcal{E}}_{k-1}) + \#\mathrm{mid}(\bar{\mathcal{E}}_{k-1}).$$

Each vertex of $\mathrm{ver}(\bar{\mathcal{E}}_{k-1})$ belongs as a vertex of a tetrahedron to *at least three* edges of $\bar{\mathcal{E}}_{k-1}$, thus $\#\mathrm{ver}(\bar{\mathcal{E}}_{k-1}) \leq \frac{1}{3} \cdot 2 \cdot \#\bar{\mathcal{E}}_{k-1}$. By means of rule (T1) we obtain $\mathrm{mid}(\bar{\mathcal{E}}_{k-1}) = \mathcal{N}_k \setminus \mathcal{N}_{k-1}$, which implies $\#\bar{\mathcal{E}}_{k-1} = \#\mathrm{mid}(\bar{\mathcal{E}}_{k-1}) = \#(\mathcal{N}_k \setminus \mathcal{N}_{k-1}) = n_k - n_{k-1}$. Thus we have $m_k \leq 5/3(n_k - n_{k-1})$ which yields the assertion. ■

Remark 2 Note that Lemma 1 does not contain any assumptions on the progression of the number of unknowns n_k.

As shown by Yserentant [33], the BPX preconditioner can be written in scaled form as $B : \mathcal{S}_j \to \mathcal{S}_j$ with

$$Br = A_0^{-1} Q_0 r + \sum_{k=0}^{j} \sum_{\psi \in \Psi_k} \frac{(r, \psi)}{a(\psi, \psi)} \psi \tag{5}$$

for any $r \in \mathcal{S}_j$. Here $(\cdot, \cdot)$ denotes a scaled L^2–scalar product and $Q_0 : \mathcal{S}_j \to \mathcal{S}_0$ the L^2–like projection associated with $(\cdot, \cdot)$.
The evaluation of the residual from the linear system associated with (4) amounts to the computation of the values (r, ψ) for the nodal basis $\psi = \psi_1^j, \ldots, \psi_{n_j}^j$ of $\mathcal{S}_j$. Thus we have to perform *restriction operations* in order to get the values for all ψ occurring in (5). Then division by $a(\psi, \psi)$ is just a diagonal scaling in a linear space of dimension $\sum_{k=0}^{j} m_k$. Finally we have to reformulate the result in the nodal basis of $\mathcal{S}_j$ leading to a related *interpolation*. A more detailed analysis, extending the arguments of Chan [12] and Griebel [19] to the non–uniform case, leads to the following factorization of the matrix representation $\boldsymbol{Br}$ of Br:

$$\boldsymbol{Br} = \boldsymbol{S} \boldsymbol{D} \boldsymbol{S}^T \boldsymbol{r}. \tag{6}$$

Here $\boldsymbol{B}$ is a $n_j \times n_j$ matrix specified below and the vectors $\boldsymbol{r}, \boldsymbol{Br} \in \mathrm{IR}^{n_j}$ have the entries

$$\boldsymbol{r} = \begin{bmatrix} (r, \psi_1^j) \\ \vdots \\ (r, \psi_{n_j}^j) \end{bmatrix} \boldsymbol{Br} = \begin{bmatrix} (Br)(x_1) \\ \vdots \\ (Br)(x_{n_j}) \end{bmatrix}.$$

The $\sum_{k=0}^{j} m_k \times \sum_{k=0}^{j} m_k$ matrix $\boldsymbol{D}$ is given by

$$\boldsymbol{D} = \begin{bmatrix} A_0^{-1} & & & \\ & 0 & & \\ & & \ddots & \\ & & & 0 \end{bmatrix} + \begin{bmatrix} \boldsymbol{D}_0 & & & \\ & \boldsymbol{D}_1 & & \\ & & \ddots & \\ & & & \boldsymbol{D}_j \end{bmatrix}$$

with $m_k \times m_k$ diagonal matrices $\boldsymbol{D}_k = \operatorname{diag}\left(a(\psi_1^k, \psi_1^k)^{-1}, \ldots, a(\psi_{m_k}^k, \psi_{m_k}^k)^{-1} \right)$, while the $n_j \times \sum_{k=0}^{j} m_k$ matrix $\boldsymbol{S}$ has the representation

$$\boldsymbol{S} = \boldsymbol{S}_{j-1}^{j} \ldots \boldsymbol{S}_1^2 \boldsymbol{S}_0^1 \tag{7}$$

where

$$\boldsymbol{S}_k^{k+1} : \mathrm{IR}^{n_k} \times \mathrm{IR}^{m_{k+1}} \times \ldots \times \mathrm{IR}^{m_j} \to \mathrm{IR}^{n_{k+1}} \times \mathrm{IR}^{m_{k+2}} \times \ldots \times \mathrm{IR}^{m_j}$$

is given by the matrix

$$\boldsymbol{S}_k^{k+1} = \begin{bmatrix} P_k^{k+1} & I_{k+1,k+1} & \\ & 0 & \\ & & I_{k+2,j} \end{bmatrix}.$$

Here $I_{k,j}$ denotes the identity of dimension $m_k + \ldots + m_j$ and $P_k^{k+1} : \mathbb{R}^{n_k} \to \mathbb{R}^{n_{k+1}}$ the matrix induced by the interpolation operator $\mathcal{S}_k \to \mathcal{S}_{k+1}$. The entry $I_{k+1,k+1}$ is responsible for keeping trace of the sum in the BPX preconditioner (5).
According to (7) the $\sum_{k=0}^{j} m_k \times n_j$ matrix $\boldsymbol{S}^T$ can be written as

$$\boldsymbol{S} = \left(\boldsymbol{S}_0^1\right)^T \left(\boldsymbol{S}_1^2\right)^T \ldots \left(\boldsymbol{S}_{j-1}^j\right)^T \tag{8}$$

where

$$\left(\boldsymbol{S}_k^{k+1}\right)^T = \begin{bmatrix} R_{k+1}^k & & \\ I_{k+1,k+1} & 0 & \\ & & I_{k+2,j} \end{bmatrix}.$$

Here the matrix

$$R_{k+1}^k = \left(P_k^{k+1}\right)^T$$

is the representation of the canonical restriction operator. The interpolations P_k^{k+1} and the restrictions R_{k+1}^k are implemented as described by Yserentant [32] in case of the hierarchical basis preconditioner. Using the corresponding result on the complexity of the hierarchical basis preconditioner, the following proposition is an immediate consequence of Lemma 1 and the representation (6).

Proposition 3 *The evaluation of $\boldsymbol{Br}$ for some vector $\boldsymbol{r}$ involves*

$$\mathcal{O}\left(\sum_{k=0}^{j} m_k\right) = \mathcal{O}(n_j)$$

floating point operations and the same order of additional storage.

Remark 4 Note that additional storage is not necessary, if we interpolate after the scaling on each level k, thus performing j V–cycles with varying depth. In this case, the computational complexity is of order $\mathcal{O}(jn_j)$

4 A–Posteriori Error Estimates

Let $u \in H_0^1(\Omega)$ denote the exact solution of (1), $u_j \in \mathcal{S}_j$ the exact solution of the approximate problem (4) and $\tilde{u}_j \in \mathcal{S}_j$ an approximate solution of (4). In particular, $\tilde{u}_j$ may result from a certain number of steps of some iterative solver applied to (4). As only $\tilde{u}_j$ is known in actual computations, we are interested in local a–posteriori error estimates for the total error $\varepsilon := \|u - \tilde{u}_j\|$ and the iteration error $\delta := \|u_j - \tilde{u}_j\|$. Here we use the energy norm $\|\cdot\| = a(\cdot,\cdot)^{1/2}$ induced by the actual bilinear form. Assuming that δ is small enough, the local contributions of the total error will be used as local error indicators in the adaptive refinement process. This concept has been introduced by Babuška and Rheinboldt [1] and is well established in adaptive finite element methods [3, 8, 14, 22, 21, 23, 30].

We will first derive a–posteriori estimates $\tilde{\varepsilon}$ of the total error ε which are reliable and efficient in the sense that

$$\gamma_0 \tilde{\varepsilon} \leq \|u - \tilde{u}_j\| \leq \gamma_1 \tilde{\varepsilon} \tag{9}$$

holds with positive constants γ_0, γ_1 independent of j. Let us briefly recall the basic approach of Deuflhard, Leinen and Yserentant [14]. Replacing $\mathcal{S}_j$ in (4) by the subspace $\mathcal{Q}_j \subset H_0^1(\Omega)$ of continuous functions which are piecewise quadratic on each tetrahedron $t \in \mathcal{T}_j$, we obtain the piecewise quadratic approximation U_j of u. Now $u - \tilde{u}_j$ is approximated by the solution $D_j = U_j - \tilde{u}_j$ of the following defect problem.

$$\text{Find } D_j \in \mathcal{Q}_j, \text{ such that } a(D_j, v) = r(v)\ , \quad v \in \mathcal{Q}_j\ , \tag{10}$$

where the residual $r \in H^{-1}(\Omega)$ is defined by $r = \ell - a(\tilde{u}_j, \cdot)$. The next assumption is crucial for the following considerations

(Q) The piecewise quadratic approximation U_j of u is of higher accuracy than u_j, i.e. we have

$$\|u - U_j\| \leq q\|u - u_j\|\ ,$$

with some fixed $q < 1$.

Recall that U_j is even of higher order than u_j, if the given data are sufficiently smooth [11]. Compare Fritzsch and Oswald [17] for the case of reentrant corners. The next lemma is a consequence of the orthogonality properties of the finite element approximations u_j and U_j [8].

Lemma 5 *Assume that* (Q) *holds and that* $\tilde{\varepsilon}$ *satisfies*

$$c\tilde{\varepsilon} \leq \|D_j\| \leq C\tilde{\varepsilon}. \tag{11}$$

Then $\tilde{\varepsilon}$ *satisfies (9) with* $\gamma_0 = c$ *and* $\gamma_1 = C\sqrt{1/(1-q^2)}$.

To find $\tilde{\varepsilon}$ with the property (11) at reasonable cost, we localize the defect problem (10) replacing $a(\cdot,\cdot)$ by some other symmetric, positive definite bilinear form $\tilde{a}(\cdot,\cdot)$ on $\mathcal{Q}_j \times \mathcal{Q}_j$. We obtain the modified defect problem:

$$\text{Find } \tilde{D}_j \in \mathcal{Q}_j, \text{ such that } \tilde{a}(\tilde{D}_j, v) = r(v)\ , \quad v \in \mathcal{Q}_j. \tag{12}$$

with solution $\tilde{D}_j$. The next Lemma states that spectrally equivalent modifications of $a(\cdot,\cdot)$ provide reliable and efficient error estimates. For an elementary proof we refer to Deuflhard, Leinen and Yserentant [14].

Lemma 6 *Assume that $\tilde{a}(\cdot,\cdot)$ is a symmetric bilinear form with the property*

$$c|v|_{\tilde{a}} \le \|v\| \le C|v|_{\tilde{a}}\ , \tag{13}$$

where $|v|_{\tilde{a}} := \tilde{a}(v,v)^{1/2}$, $v \in \mathcal{Q}_j$. Then the estimates (11) hold with $\tilde{\varepsilon} := |\tilde{D}_j|_{\tilde{a}}$.

In view of these general results, we are left with the problem to find a spectrally equivalent preconditioner $\tilde{a}(\cdot,\cdot)$ for $a(\cdot,\cdot)|_{\mathcal{Q}_j\times\mathcal{Q}_j}$. Recall that $\mathcal{E}_j$ is denoting the interior edges of $\mathcal{T}_j$. Then we make use of the two–level splitting

$$\mathcal{Q}_j = \mathcal{S}^L \oplus \mathcal{S}^Q$$

consisting of $\mathcal{S}^L := \mathcal{S}_j$ and $\mathcal{S}^Q := \operatorname{span}\{\mu_e |\ e \in \mathcal{E}_j\}$, where the quadratic bubbles $\mu_e \in \mathcal{Q}_j$ are defined by $\mu_e(p) = 0$, $p \in \mathcal{N}_j$, and $\mu_e(\text{midpoint of } \bar{e}) = \delta_{e,\bar{e}}$, $\bar{e} \in \mathcal{E}_j$ (Kronecker delta). Note that this splitting is independent of the space dimension. Utilizing the representation $v = v_L + \sum_{e\in\mathcal{E}_j} v_e\mu_e$, $v \in \mathcal{Q}_j$, the quadratic form $\tilde{a}(\cdot,\cdot)$ is defined by

$$\tilde{a}(v,w) = b(v^L, w^L) + \sum_{e\in\mathcal{E}_j} v_e w_e a(\mu_e,\mu_e)\ , \quad v,w \in \mathcal{Q}_j. \tag{14}$$

Here $b(\cdot,\cdot) := (B\cdot,\cdot)$ denotes the symmetric bilinear form induced by the BPX preconditioner considered in the preceding section. We can state the main result of this section.

Theorem 1 *Assume that* (Q) *is satisfied and that $\tilde{D}_j$ is the solution of the localized defect problem (12) with $\tilde{a}(\cdot,\cdot)$ defined by (14). Then the total error estimate $\tilde{\varepsilon} := |\tilde{D}_j|_{\tilde{a}}$ is efficient and reliable in the sense that*

$$\gamma_0\, \tilde{\varepsilon} \le \|u - \tilde{u}_j\| \le \gamma_1\, \tilde{\varepsilon} \tag{15}$$

holds with $\gamma_0 = c$, $\gamma_1 = C\sqrt{1/(1-q^2)}$ and constants c, C depending only on the shape regularity of $\mathcal{T}_0$ and the ellipticity of $a(\cdot,\cdot)$.

Proof. In view of Lemma 5, Lemma 6 and uniform bound of the condition number related to the BPX preconditioner (see Oswald [25], Dahmen and Kunoth [13], Bornemann and Yserentant [9] and the included references), we only have to show that $a(\cdot,\cdot)$ and $a^\star(\cdot,\cdot)$ defined by

$$a^\star(v,w) = a(v^L, w^L) + \sum_{e\in\mathcal{E}_j} v_e w_e a(\mu_e,\mu_e)\ , \quad v,w \in \mathcal{Q}_j\ ,$$

are spectrally equivalent with constants depending only on the shape regularity of $\mathcal{T}_0$ and the ellipticity of $a(\cdot,\cdot)$. By the triangle inequality and Cauchy's inequality we have

$$a_t(v,v) \le (\|v^L\| + \sum_{e\in\mathcal{E}_j} \|v_e\mu_e\|)^2 \le 7\ a_t^\star(v,v), \tag{16}$$

where the subscript t indicates the restriction of the bilinear form to some tetrahedron $t \in \mathcal{T}_j$. The converse estimate

$$a_t^\star(v,v) \le C\ a_t(v,v) \tag{17}$$

follows by the usual affine transformation technique, exploiting the ellipticity of $a(\cdot,\cdot)$. ∎

By the definition of $\tilde{a}(\cdot,\cdot)$ the contributions $\eta_e = (\tilde{D}_e)^2 a(\mu_e,\mu_e)$ of the edges $e \in \mathcal{E}_j$ to the total error are completely decoupled. The only time consuming part in the computation of η_e is the evaluation of $a(\mu_e,\mu_e)$, $e \in \mathcal{E}_j$ and of the residual $r|_{\mathcal{Q}_j}$. We will use the local contributions η_e, $e \in \mathcal{E}_j$ as local error indicators in the adaptive refinement process. In particular, a tetrahedron $t \in \mathcal{T}_j$ is marked for refinement, if the value η_e of at least one of its edges e exceeds a certain threshold $\sigma\bar{\eta}$. Here $\bar{\eta}$ is a guess of the maximal local error arising on the next level in case of uniform refinement and $\sigma < 1$ is a safety factor. In the numerical examples reported in the final section, $\bar{\eta}$ is computed by local extrapolation [1, 7] and we chose $\sigma = 0.5$.

To obtain an estimate $\tilde{\delta}$ for the iteration error, we use the linear defect problem

$$\text{Find } \tilde{d}_j \in \mathcal{S}_j \text{ such that } b(\tilde{d}_j, v) = r(v)\ , \quad v \in \mathcal{S}_j \tag{18}$$

We only have to rewrite the spectral equivalence of the BPX preconditioner to prove the following Theorem.

Theorem 2 *Let $\tilde{d}_j$ be the solution of the linear defect problem (18). Then the iterative error estimate $\tilde{\delta} := |\tilde{d}_j|_b$ is reliable and efficient in the sense that the estimates*

$$\beta_0\tilde{\delta} \le \|u_j - \tilde{u}_j\| \le \beta_1\tilde{\delta} \tag{19}$$

hold with constants β_0, β_1 depending only on the shape regularity of $\mathcal{T}_0$ and the ellipticity of $a(\cdot,\cdot)$.

Remark 7 The evaluation of (18) represents the preconditioning of the residual which takes place in each step of the preconditioned cg–iteration. Hence $\tilde{\delta}$ is available without additional computational work.

Remark 8 Using the splitting $\tilde{D}_j = \tilde{D}_j^L = \tilde{D}_j^Q$ we immediately have $\tilde{D}_j^L = \tilde{d}_j^L$. Nevertheless the contributions from inexact solution and discretization are not completely decoupled, as $\tilde{u}_j$ enters the right hand side of the local defect problems for the quadratical part $\tilde{d}^Q$.

To preserve the over all accuracy by the iterative solution of (4), the iteration should be continued until the related total error $\varepsilon_j = \|u - \tilde{u}_j\|$ is of the order of the discretization error $\|u - u_j\|$. We assume that the discretization error is bounded in terms of the number of unknowns $n_j = \#\mathcal{N}_j$.

(D) The estimate

$$\|u - u_j\| \le c\, n_j^{-1/3}$$

holds with a constant c independent of j.

In case of a uniform mesh with mesh size $h = n_j^{-1/3}$ the assumption (D) is reducing to the well–known a priori error estimate of the H^1–error. For related results in the nonuniform case we refer to Babuška, Kellogg and Pitkäranta [2].

The following proposition gives a sufficient criterion to ensure the same asymptotic behavior of the total error and the discretization error.

Proposition 9 *Assume that (D) is satisfied. Let* $\delta_0 = 0$ *and assume that*

$$\delta_k \le \rho\, \left(\frac{n_{k-1}}{n_k}\right)^{1/3} \varepsilon_{k-1} \tag{20}$$

holds for $1 \le k \le j$ *with some fixed* $\rho < 1$*, then we have the estimate*

$$\varepsilon_j \le c \frac{1}{1-\rho} (n_j)^{-1/3}. \tag{21}$$

Proof. The assertion follows by inductive application of (20). ∎

Note that the accuracy may still be deteriorated in exceptional cases when the discretization error behaves better than expected in (D).

As only the a–posteriori estimates $\tilde{\delta}$ and $\tilde{\varepsilon}_{j-1}$ are available in actual computations, we replace (20) by the stopping criterion

$$\tilde{\delta}_j \le \rho\, \left(\frac{n_{j-1}}{n_j}\right)^{1/3} \tilde{\varepsilon}_{j-1}\,, \quad j \ge 1\,, \tag{22}$$

starting with the direct solution on level 0. In this case the order of accuracy is preserved in the sense of (21) if ρ satisfies $\rho < \gamma_0/\beta_1$ with γ_0 and β_1 taken from (15) and (19). We chose $\rho = 0.01$ for our numerical experiments.

5 Numerical Results

The modules described in the preceding sections are implemented by suitable extension of the adaptive finite element code KASKADE [14, 16, 27, 28]. For details we refer to the 3–D ELLKASK Programmer's Manual [15]. In this section we report the numerical results for a model problem involving a corner singularity and the so–called Bio–Heat–Transfer equation (BHT equation) arising in clinical hyperthermia.

Example 1: Corner Singularity. We consider the homogeneous boundary value problem for the Laplacian arising from the choice $a_{i,j} = \delta_{i,j},\ i,j = 1,\ldots,3$ (Kronecker delta) and

$$\ell(v) = \int_\Omega v \, d\boldsymbol{x},\ v \in H_0^1(\Omega),$$

in our basic problem (1). The computational domain Ω is given by

$$\Omega = (-1,1) \times (-1,1) \times (-1,1) \setminus [0,1) \times [0,1) \times [0,1),$$

and we use the initial triangulation $\mathcal{T}_0$ depicted in Figure 9.

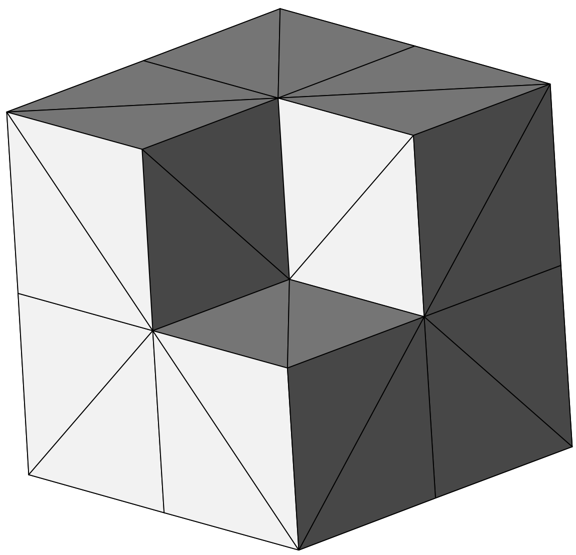

Figure 9. Surface of the Initial Triangulation of Ω

To study the effect of preconditioning, we perform four uniform refinement steps and solve the resulting discrete problems iteratively by the conjugate gradient method using the initial iterate $u_j^{(0)} = 0$ and the stopping criterion

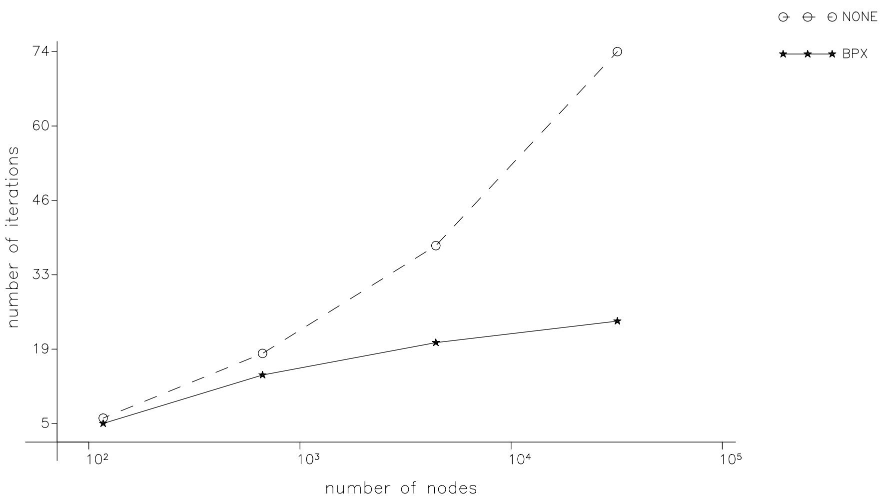

Figure 10. BPX Preconditioning on Uniform Triangulations

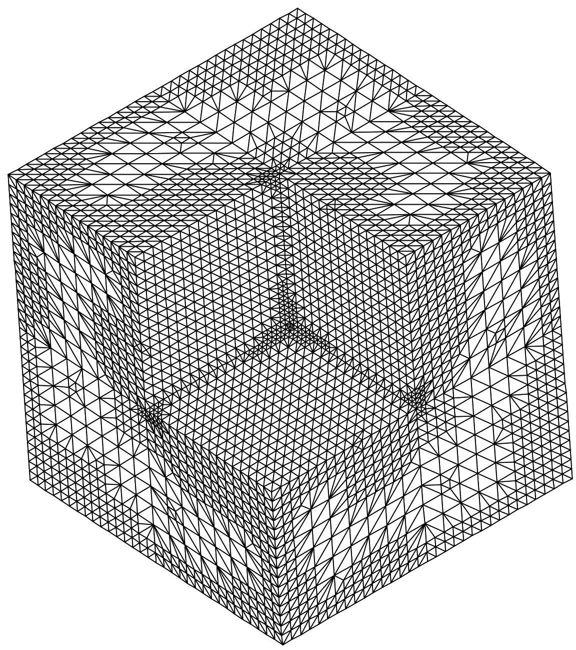

Figure 11. Surface of the Triangulation $\mathcal{T}_6$ on Refinement Level 7

$\tilde{\delta}_j < 1.E - 12$ with $\tilde{\delta}_j$ obtained from (18). Figure 10 shows the number of iteration steps comparing the BPX preconditioner with the unpreconditioned case.

As expected, the unpreconditioned conjugate gradient method results in an exponential growth of the number of iterations, while the BPX preconditioner

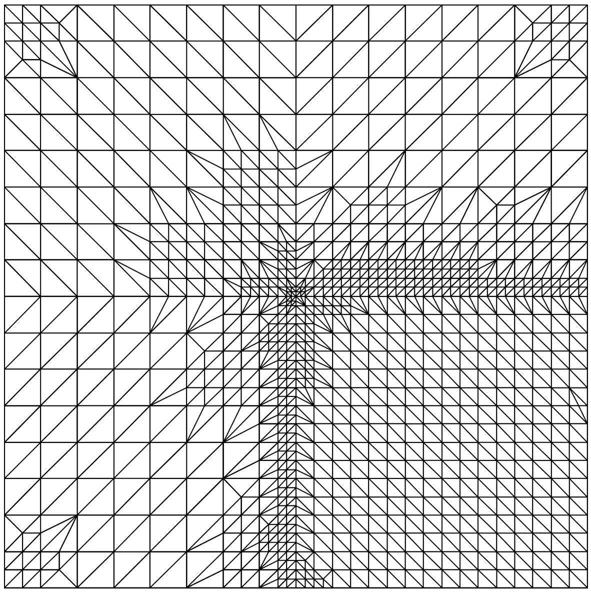

Figure 12. Clipping of the Triangulation $\mathcal{T}_6$ at z=0

tends to be asymptotically optimal with increasing j.

level	depth	N	BPX prec. [iterations]	t_p $[s * 10^{-4}]$
1	1	117	1	1.4
2	2	463	3	1.4
3	3	938	1	2.1
4	4	4281	4	2.4
5	4	5789	1	2.7
6	5	6948	1	3.0
7	6	17526	2	3.0

Table 1. Iteration History for Example 1

Now we apply the adaptive procedure described in the preceding section to obtain the sequence of triangulations $\mathcal{T}_1, \ldots \mathcal{T}_6$ from $\mathcal{T}_0$. Of course, we used the approximation $\tilde{u}_{j-1} \in \mathcal{S}_{j-1} \subset \mathcal{S}_j$ from the preceding level as an initial guess for the iterative solution. Together with the stopping criterion (22) and the rapid convergence of the preconditioned cg–method this leads to a very moderate number of iterations. A detailed iteration history is given in Table 1. Here t_p denotes the elapsed CPU – time for the iteration process

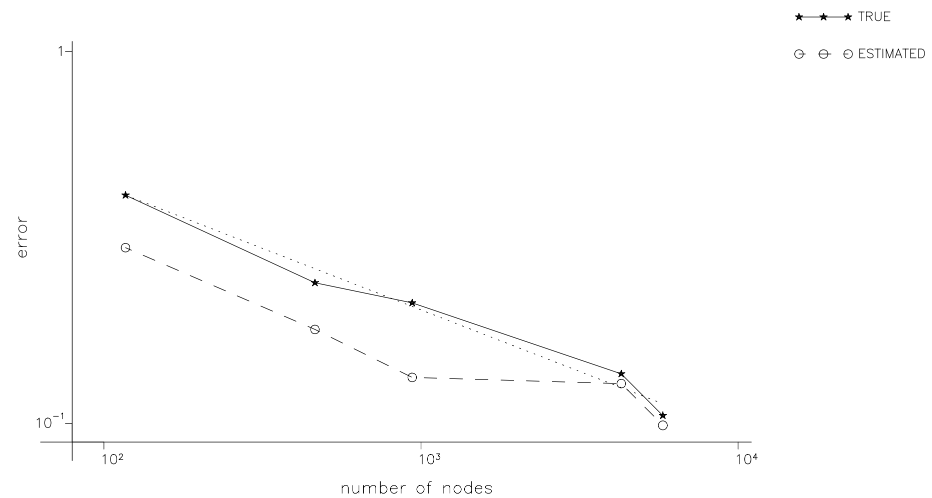

Figure 13. Discretization Error and A–Posteriori Error Estimation

over the number of iterations and nodal points. Observe that t_p saturates with increasing j, as predicted in Proposition 3.

Finally, the Figures 11 and 12 illustrate the final triangulation $\mathcal{T}_6$ showing the expected concentration of nodes in the neighborhood of the singularities.

The development of the discretization error and the a–posteriori error estimate resulting from (12) is depicted in Figure 13. To compute the "exact" error, we performed a uniform refinement on level 5 (not on level 7 for lack of memory) and determined the difference to the corresponding solution. For a comparison, the dotted line shows the optimal asymptotic behavior $\mathcal{O}(n_j^{-1/3})$ of the error which is well–known from approximation theory. Note that these results confirm our assumption (D) mentioned in Section 4.

Example 2: The Bio–Heat–Transport Equation. In order to demonstrate the applicability of our code to real life problems combining various difficulties as complex geometry and/or discontinuous coefficients, we consider a problem arising in hyperthermia.

Hyperthermia is a therapy based on the observation that local heating may slow down or even stop the growth of a tumor, especially if it is applied in combination with other methods like chemotherapy or radiotherapy. The deep heating of the tissue is obtained by an electric field which is generated by pairs of antennas. The antennas are either fixed on the skin or implanted in the tissue itself. Of course the position of the antennas and frequency of the electric field have to be chosen properly to achieve a local heating of the tumor without the surrounding tissue [31]. This requires the efficient and

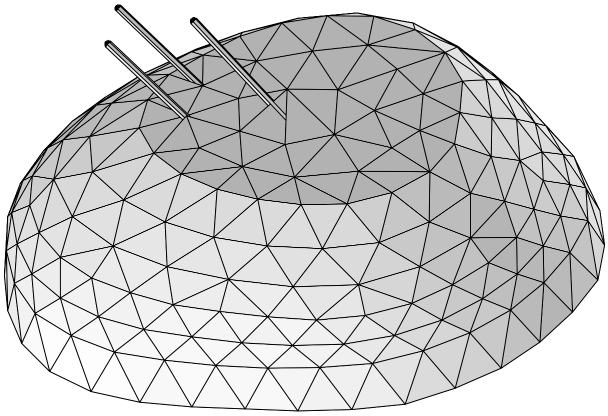

Figure 14. Surface of the Initial Triangulation of the Skull

level	depth	N	BPX prec. [iterations]	t_p $[s * 10^{-4}]$
1	1	2085	4	2.6
2	2	2354	2	3.4
3	3	3234	2	3.4
4	3	3825	2	3.3
5	4	7562	3	3.2
6	4	12167	3	3.1
7	5	16313	2	3.3

Table 2. Iteration History for Example 2

robust solution of the BHT equation: [26]

$$\text{Find } u \in H_0^1(\Omega) \text{ such that } a(u,v) + (qu,v) = (f,v), \quad v \in H_0^1(\Omega), \tag{23}$$

modeling the temperature distribution u for a given electric field $\boldsymbol{E}$. Note that $\boldsymbol{E}$ together with nonhomogeneous Dirichlet boundary conditions is incorporated in the source term f, while the temperature flow is modeled by the bilinear form $a(\cdot,\cdot)$ and q. The coefficients a_{ij} and q are taken piecewise constant on different tissues. We refer to Seebaß [29] for a more detailed explanation and the numerical data of the following example.

We consider the heating of a tumor which is contained in a human skull by the

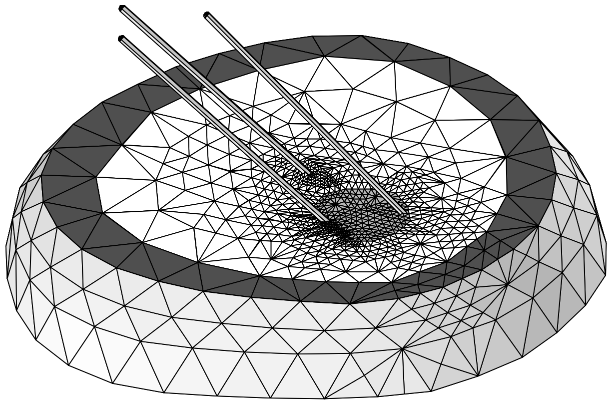

Figure 15. Clipping of the Triangulation $\mathcal{T}_5$ on Refinement Level 7

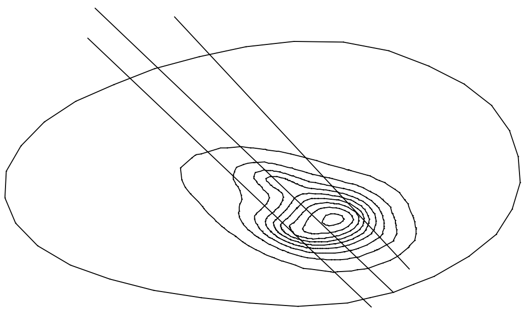

Figure 16. Isolines of Temperature on the Clipping Plane

electric field resulting from three implanted antennas. A suitable description of the computational domain Ω is obtained by computer tomography. Figure 14 is showing the surface of Ω and the initial triangulation $\mathcal{T}_0$ which is given by Seebaß [29]. Note that $\mathcal{T}_0$ is chosen such that different tissues as bone, brain and tumor belong to different tetrahedra. Finally, the additional Helmholtz term appearing in (23) has to be incorporated properly in the BPX preconditioner as proposed by Bornemann [8]. Performing 7 adaptive refinement steps we obtain the iteration history reported in Table 2. Again the results confirm the efficiency of the proposed multilevel method and its implementation. As expected, the refinement concentrates on the neighborhood of the antennas and the tumor in the interior of the skull where we have high gradients of the temperature. This is illustrated by Figures 15 and 16 showing the final triangulation $\mathcal{T}_5$ and the level curves of the temperature on some clipping plane. Here the different tissues are indicated by black (bone), white (brain) and grey (tumor).

All computations have been carried out on a SUN Sparc IPX.

Acknowledgments The authors are deeply indebted to P. Deuflhard for initiating and encouraging their work on adaptive multilevel methods. Sincere thanks to R. Roitzsch for his invaluable help extending the data structures of KASKADE and to M. Seebaß for providing the initial mesh for the numerical example from hyperthermia. The figures have been generated with the help of the graphical environment GRAPE which is developed and distributed by the Sonderforschungsbereich 256 at the University of Bonn, Germany.

References

1. I. Babuška, W.C. Rheinboldt: *Estimates for Adaptive Finite Element Computations.* SIAM J. Num. Anal. **15**, p. 736–754 (1978)

2. I. Babuška, R.B. Kellogg, J. Pitkäranta: *Direct and Inverse Error Estimates for Finite Elements with Mesh Refinements.* Numer. Math. **33**, p. 447–471 (1979)

3. R.E. Bank: *PLTMG – A Software Package for Solving Elliptic Partial Differential Equations. User's Guide 6.0.* SIAM, Philadelphia (1990)

4. R.E. Bank, A.H. Sherman, H. Weiser: *Refinement Algorithms and Data Structures for Regular Local Mesh Refinement.* Scientific Computing, R. Stepleman et al. (eds.), Amsterdam: IMACS North–Holland, p. 3–17 (1983)

5. E. Bänsch: *Local Mesh Refinement in 2 and 3 Dimensions.* IMPACT Comput. Sci. Engrg. **3**, p. 181–191 (1991)

6. J. Bey: *Analyse und Simulation eines Konjugierte–Gradienten–Verfahrens mit einem Multilevel–Präkonditionierer zur Lösung dreidimensionaler, elliptischer Randwertprobleme für massiv parallele Rechner.* Diplomarbeit, RWTH Aachen (1991)

7. F. Bornemann: *An Adaptive Multilevel Approach to Parabolic Equations in Two Space Dimensions.* Dissertation, FU Berlin (1991)

8. F. Bornemann: *An Adaptive Multilevel Approach to Parabolic Equations III.* IMPACT Comput. Sci. Engrg. **4**, p. 1–45 (1992)

9. F. Bornemann, H. Yserentant: *A Basic Norm Equivalence in the Theory of Multilevel Methods.* To appear in Numer. Math. (1992)

10. J.H. Bramble, J.E. Pasciak, J. Xu: *Parallel Multilevel Preconditioners.* Math. Comp., **55**, p. 1–22 (1990)

11. P. G. Ciarlet: *The Finite Element Method for Elliptic Problems.* North–Holland, Amsterdam (1980)

12. T. Chan: *private communication.* (1991)

13. W. Dahmen, A. Kunoth: *Multilevel Preconditioning.* To appear in Numer. Math. (1992)

14. P. Deuflhard, P. Leinen, H. Yserentant: *Concepts of an Adaptive Hierarchical Finite Element Code.* IMPACT Comput. Sci. Engrg. **1**, p. 3–35 (1989)

15. B. Erdmann, R. Roitzsch: *3–D ELLKASK Programmers Manual 1.0* . To appear as Technical Report, Konrad–Zuse–Zentrum Berlin (ZIB)

16. B. Erdmann, R. Roitzsch, F. Bornemann: *KASKADE Numerical Experiments.* Technical Report TR 91–1, Konrad–Zuse–Zentrum Berlin (ZIB) (1991)

17. R. Fritzsch, P. Oswald: *Zur optimalen Gitterwahl bei Finite–Elemente–Approximationen.* Wiss. Zeitschr. d. TU Dresden **37**, p. 155–158 (1988)

18. M. E. Go Ong: *Hierarchical Basis Preconditioners for Second Order Elliptic Problems in Three Dimensions.* Ph.D. Thesis, University of California, Los Angeles (1989)

19. M. Griebel: *Multilevel Algorithms Considered as Iterative Methods on Semidefinite Systems.* TUM–I9143, SFB–Bericht Nr. 342/29/91A TU München (1991), to appear in SIAM J. Sci. Stat. Comp.

20. W. Hackbusch:*Multi–Grid Methods and Applications.* Springer (1985)

21. R.H.W. Hoppe, R. Kornhuber: *Adaptive Multilevel Methods for Obstacle Problems.* Preprint SC 91–16, Konrad–Zuse–Zentrum Berlin (ZIB) (1991)

22. C. Johnson: *Numerical Solutions of Partial Differential Equations by the Finite Element Method.* Cambridge University Press, Cambridge (1987)

23. P. Leinen: *Ein schneller adaptiver Löser für elliptische Randwertprobleme.* Dissertation, Dortmund (1990)

24. Ch.K. Mesztenyi, W.C. Rheinboldt: *NFEARS: A Nonlinear Adaptive Finite Element Solver.* Report ICMA–87–113 Department of Mathematics and Statistics, University of Pittsburgh (1987)

25. P. Oswald: *On Discrete Norm Estimates Related to Multilevel Preconditioners in the Finite Element Method.* In: Proceedings of the International Conference on the Constructive Theory of Functions, Varna 1991 (to appear)

26. H.H. Pennes: *Analysis of Tissue and Arterial Blood Temperatures in the Resting Human Forearm.* J. Appl. Physiol. **1**, p. 93–122 (1948)

27. R. Roitzsch: KASKADE *User's Manual.* Technical Report TR 89-4, Konrad–Zuse–Zentrum Berlin (ZIB) (1989)

28. R. Roitzsch: KASKADE *Programmer's Manual.* Technical Report TR 89-5, Konrad–Zuse–Zentrum Berlin (ZIB) (1989)

29. M. Seebaß : *3D-Computersimulation der interstitiellen Mikrowellen-Hyperthermie von Hirntumoren.* Bericht Nr. 1/90, Inst. f. Radiologie und Pathophysiologie, Deutsches Krebsforschungszentrum Heidelberg (1990)

30. B. Szabó, I.Babuška: *Finite Element Analysis.* J. Wiley & Sons, New York (1991)

31. P. Wust, J. Nadobny, R. Felix, P. Deuflhard, W. John, A. Louis: *Numerical Approaches to Treatment Planning in Deep RF–Hyperthermia.* Strahlenther. Onkol. **165**, p. 751–757 (1989)

32. H. Yserentant: *On the Multilevel Splitting of Finite Element Spaces.* Numer. Math. **49**, p. 379–412 (1986)

33. H. Yserentant: *Two Preconditioners Based on the Multilevel Splitting of Finite Element Spaces.* Numer. Math. **58**, p. 163–184 (1990)

34. S.Zhang: *Multilevel Iterative Techniques.* Ph.D. Thesis, Pennsylvania State University (1988)